# Low-Threshold Subharmonic Generation in Composite Structures with Cantor-Like Code

A. Alippi,[(1),(2)] G. Shkerdin,[(1),(3)] A. Bettucci,[(1)] F. Craciun,[(1),(2)] E. Molinari,[(1),(a)] and A. Petri[(1)]

[(1)]*Consiglio Nazionale delle Ricerche (CNR), Istituto di Acustica "O.M. Corbino," Via Cassia 1216, I-00189 Roma, Italy*

[(2)]*Dipartimento di Energetica, Università degli Studi di Roma "La Sapienza," Roma, Italy*

[(3)]*Institute of Radio Engineering and Electronics, Academy of Sciences, Moscow, Russia*

(Received 3 August 1992)

We show experimental evidence of extremely low thresholds for subharmonic generation of ultrasonic waves in one-dimensional artificial piezoelectric plates with Cantor-like structure, as compared to the corresponding homogeneous and periodical plates. The origin of this apparent anomaly is theoretically investigated by studying anharmonic coupling between normal modes. We demonstrate that the large enhancement of nonlinear interaction results from the more favorable frequency and spatial matching of coupled modes (fractons and phonons) in the Cantor-like structure, with no need to invoke anomalous modifications of the nonlinear elastic constants.

PACS numbers: 43.25.+y, 62.65.+k, 63.20.Pw, 63.50.+x

In recent years, harmonic properties of disordered and fractal structures have been widely studied both experimentally and theoretically [1]. As concerns the anharmonic regime, however, detailed experimental studies of coupling processes between different vibrational modes are still lacking in these systems. Indeed, while it was pointed out that anharmonic effects may have a special relevance if the interaction involves extended and localized modes—as in amorphous or glassy systems [2]—the available data are limited to frequency-integrated quantities such as thermal conductivity [2]. This is probably due to severe difficulties in directly probing individual coupling processes in microscopically complex materials.

On the other hand, in macroscopic resonators nonlinearity is known to couple normal modes, so that a net energy flow is established from a driving frequency to higher (harmonic) or to lower (subharmonic) frequencies [3]. In particular, subharmonic generation is a threshold phenomenon, which has been reported in the past in ultrasonic resonators [4] and more recently in periodic media [5]. A macroscopic resonator with self-similar structure is therefore a good candidate as a simple model system whose dynamics retains the major features of the above-mentioned complex materials—namely, the existence of localized and extended mode regimes—while allowing direct experimental detection of nonlinear coupling effects between selected vibrational modes, with known spatial behavior, through the investigation of subharmonic thresholds in the excitation power.

Recently [6], we reported on the linear acoustic behavior of an artificial one-dimensional piezoelectric composite plate with hierarchical code. The existence of localized (fracton) and extended (phonon) vibrational regimes was experimentally demonstrated. In the present Letter, we show that indeed subharmonic generation can be obtained in this fractal structure, and that anomalously low thresholds are found with respect to similar homogeneous and periodical structures. Moreover, we directly measure the surface displacement profiles of the coupled modes, whose frequency and spatial overlap enter the theoretical expression of the threshold. We demonstrate that the observed anomalous enhancement of anharmonic interaction is due to the fact that—for a given fundamental mode—much more favorable frequency and spatial matching conditions are met with respect to homogeneous and periodical structures, and no anomalous modification of nonlinear elastic constants must be invoked to explain our experiments. Thus, the "disturbing" assumptions [7] previously introduced to explain anharmonic effects in amorphous materials seem to be not needed.

Our sample (inset of Fig. 1) is a composite plate formed by alternating elements of PZT (lead zirconate titanate) piezoelectric ceramic (grey regions) and epoxy resin (black regions) following a triadic Cantor-like se-

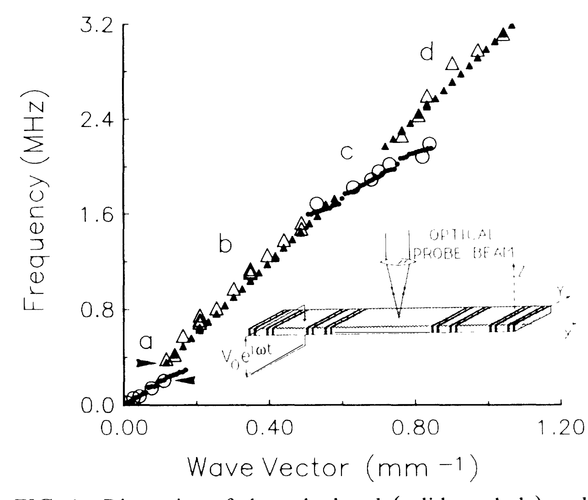


FIG. 1. Dispersion of the calculated (solid symbols) and the experimental (open symbols) normal modes of the Cantor-like sample sketched in the inset. Circles represent extended modes [phonon regimes ($a$ and $c$)], while triangles represent localized modes [fracton regimes ($b$ and $d$)]. For the definition of the wave vector $q$, see Ref. [10]. The arrows mark the modes involved in the anharmonic coupling (Fig. 2, curve $a$), whose experimental and theoretical displacement profiles are shown in Figs. 3 and 4.

 

quence up to the fourth generation. The sample parameters are such that scalar propagation along $x$ occurs in the frequency range of interest [6,8,9]. Normal modes are excited by applying an ac voltage $V=V_0\exp(i\omega t)$ to metal electrodes deposited on both sides of the sample; their frequencies $\omega$ are identified from peaks of the admittance curve in the linear regime ($V_0 \cong 0.1$ V). Surface displacement profiles are then measured by an interferometric laser probe [6,8]. The resulting dispersion is shown in Fig. 1 [10]. Different frequency ranges, as identified in Ref. [6], are labeled $a$ and $c$ for phonon regimes, and $b$ and $d$ for fracton regimes. The theoretical dispersion is also displayed in Fig. 1, showing excellent agreement [10].

The nonlinear response of the system is studied by applying a voltage $V$ of frequency $\omega$ close to the frequency $\omega_n$ of a normal mode $n$, and by measuring the frequency spectrum of the excited vibrations as a function of the amplitude $V_0$. If $V_0$ is increased above a threshold value $V_{\text{th}}$, sudden $\omega/2$ subharmonic generation is observed ($V_{\text{th}}$ is found to depend on the specific modes). The amplitude of the $\omega/2$ subharmonic was measured as a function of the applied voltage amplitude for the Cantor-like sample, as well as for a periodical sample and a homogeneous piezoelectric plate [11]. The results are shown in Fig. 2. *While typical values of the lowest threshold voltages observed in the Cantor-like sample are* $V_{th} \cong 3$-$5$ *V, much higher values* ($V_{th} \cong 25$ *V) are obtained for the other samples.*

To explain this evidence, we used the following theoretical model for subharmonic thresholds in our samples [12]. We start by introducing anharmonic terms in the one-dimensional wave equation:

$$\rho \frac{\partial^2 u(x,t)}{\partial t^2} = \frac{\partial[\sigma(x,t)+F(x,t)]}{\partial x}, \tag{1}$$

where $u$ and $\sigma$ are displacement and stress, respectively, $\rho$

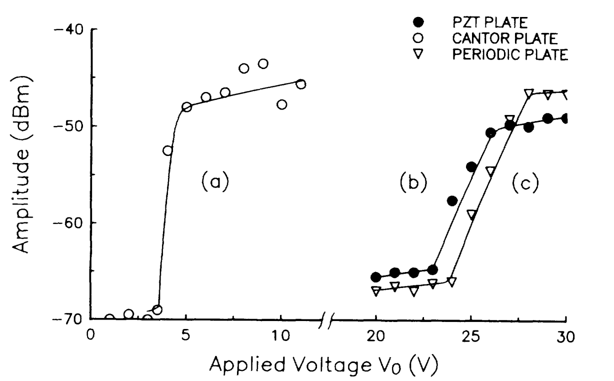


FIG. 2. Low-threshold subharmonic generation in the Cantor-like sample (curve $a$) as compared with the corresponding homogeneous ($b$) and periodic ($c$) plates. The fundamental mode is at frequency $\omega_n = 385.5$ kHz for the Cantor-like sample; $\omega_n = 260$ and 220 kHz for the homogeneous and periodic plates, respectively.

is the mass density, and $F=F_{\text{abs}}+F_e+F_{\text{NL}}$ includes not only the second-order elastic term $F_{\text{NL}}$, but also damping ($F_{\text{abs}}$) and source ($F_e$) factors. If $F(x,t)$ is small, the total stress $\sigma'(x,t)=\sigma(x,t)+F(x,t)$ can be expanded in terms of normal modes of the structure:

$$\sigma'(x,t) = \sum_j C_j(t) e^{-i\omega_j t} \sigma^{(j)}(x) + F(x,t). \tag{2}$$

With the assumption that the expansion coefficients $C_j(t)$ vary slowly with time, such that $\Delta C_j/C_j \ll 1$ within an acoustic period, the time-dependent amplitude equation for the $n$th mode becomes

$$\frac{dC_n}{dt} = \frac{ie^{i\omega_n t}}{2\omega_n} \int_0^L u^{(n)}(x) \frac{\partial F(x,t)}{\partial x} dx, \tag{3}$$

where $u^{(n)}(x)$ is the normalized displacement and the integral is taken over the resonator length $L$. In an elastic nonlinear plate excited at frequency $\omega$, Eq. (3) becomes

$$\frac{dC_n}{dt} = -\alpha_n C_n + \frac{ie^{i(\omega_n-\omega)t}}{2\omega_n} V_0 I_e^{(n)} + \frac{ie^{i\omega_n t}}{2\omega_n} \int_0^L u^{(n)}(x) \frac{\partial F_{\text{NL}}(x,t)}{\partial x} dx, \tag{4}$$

where the first and the second terms come from $F_{\text{abs}}$ and $F_e$, and the third is due to the nonlinear part $F_{\text{NL}}$. $\alpha_n$ is the absorption coefficient of the $n$th mode, while

$$I_e^{(n)} = \frac{1}{h} \int_0^L u^{(n)}(x) \frac{\partial}{\partial x} \frac{d_{31}(x)}{S_{11}^E(x)} dx \tag{5}$$

is the excitation term, with $d_{31}(x)$ and $S_{11}^E(x)$ nonuniform piezoelectric and elastic compliance constants, and $h$ the plate thickness. $F_{\text{NL}}$ is the nonlinear longitudinal stress:

$$F_{\text{NL}}(x,t) = \sum_{kl} c_{111}(x) \frac{\partial u^{(k)}(x)}{\partial x} \frac{\partial u^{(l)}(x)}{\partial x}, \tag{6}$$

where $c_{111}(x)$ is the appropriate third-order elastic constant. This last term can give rise to subharmonics if $\omega_k + \omega_l = \omega_n$. In the following we only consider half-frequency subharmonics ($\omega_k = \omega_l = \omega_n/2$), and adopt the two-mode approximation (only two eigenmodes with frequencies $\omega_n$ and $\omega_m$ are close to $\omega$ and $\omega/2$, respectively). By imposing the stability condition on the rate equation (4), the threshold amplitude for subharmonic generation is finally obtained:

$$V_{\text{th}} = D(\omega)/I_e I_o. \tag{7}$$

Besides the excitation term $I_e$, the threshold thus depends on

$$I_o = \int_0^L c_{111}(x) \left[ \frac{\partial u^{(m)}(x)}{\partial x} \right]^2 \frac{\partial u^{(n)}(x)}{\partial x} dx, \tag{8}$$

the overlap integral between the strain fields of the fundamental ($n$) and subharmonic ($m$) modes. $D(\omega)$ is a factor which depends on the absorption coefficients $\alpha$, on the

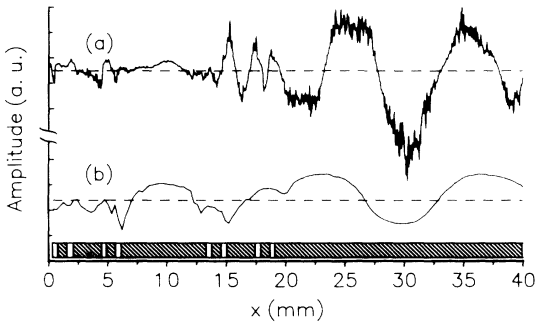


FIG. 3. Experimental displacement profiles of the normal modes (a) $\omega_n = 385.5$ kHz and (b) $\omega_m \cong \omega_n/2$ of the Cantor-like sample. (The structure is sketched at the bottom; only half of the $x$ range is shown.) The anharmonic coupling between these two modes, which is responsible for the subharmonic generation of Fig. 2, curve $a$ is favored by the relatively large spatial overlap between the square of the subharmonic displacement (b) and the displacement of the fundamental mode (a) in the region where the fracton mode (a) extends.

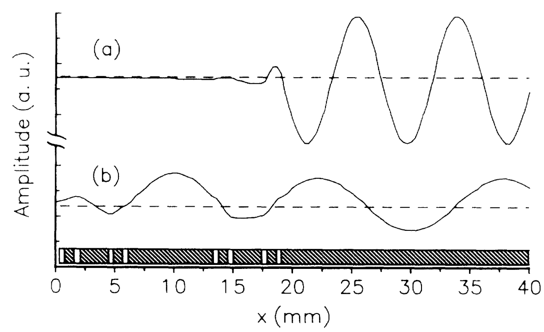


FIG. 4. Calculated amplitude of the surface displacement profiles of the same normal modes as in Fig. 3: (a) $\omega_n = 385.5$ kHz and (b) $\omega_m \cong \omega_n/2$ of the Cantor-like sample. (The structure is sketched at the bottom; only half of the $x$ range is shown.)

mismatch between the applied frequency $\omega$ and $\omega_n$, and on the mismatch between $\omega/2$ and $\omega_m$:

$$D(\omega) = \omega^2[\alpha_n^2 + (\omega - \omega_n)^2]^{1/2}[\alpha_m^2 + (\omega/2 - \omega_m)^2]^{1/2}. \tag{9}$$

We have used Eq. (7) to calculate the threshold amplitudes for our Cantor-like structure as well as for a periodic and a homogeneous piezoelectric plate. The eigenmode frequencies and profiles were calculated as in Refs. [6,8], in excellent agreement with experiments (compare, e.g., Figs. 3 and 4). Effective absorption coefficients were obtained from the resonance widths in the admittance spectrum of the structures [$\alpha(\omega) \propto \omega$; $\alpha \cong 10^3\ \mathrm{s}^{-1}$ at $\omega = 200$ kHz]. The third-order elastic constants for ceramic and resin are taken as $c_{111} = -100 c_{11} = -12.6 \times 10^{12}\ \mathrm{N/m^2}$ [9] and $c_{111} = 9 c_{11} = 4.9 \times 10^{10}\ \mathrm{N/m^2}$ [13], respectively; for the piezoelectric stress constant we have $d_{31}/S_{11}^E = 16.6\ \mathrm{C/m^2}$ [9].

The lowest calculated threshold values are $\sim 5$ V for Cantor, $\sim 26$ V for homogeneous, and $\sim 30$ V for periodical samples. Very good agreement is found with the experimental values of Fig. 2, except for the periodical composite sample where the higher calculated threshold is due to the small value of the excitation term $I_e$: Experimentally $I_e$ is higher than predicted, probably due to small irregularities in the layer widths.

For a more detailed understanding of these differences, we recall the main result of our model [Eq. (7)]: Given a normal mode $\omega_n$, for excitation at $\omega = \omega_n$, the value of the expected threshold $V_{\mathrm{th}}$—i.e., the ability of generating the $\omega/2$ subharmonic—is determined by the existence of a normal mode $\omega_m$ with (i) small frequency mismatch $(\omega_m - \omega/2)$ and (ii) large spatial overlap between the fundamental and subharmonic strain fields. In Figs. 5(a)-5(c) we plot the overlap integrals $I_o$ between the fundamental mode and the eigenmodes around $\omega/2$ for the three cases of Fig. 2. Clearly, the Cantor-like structure presents several modes very close to $\omega/2$ which have high spatial overlap with the fundamental mode; this is due to the fact that here the fundamental mode is a localized fracton and several extended modes exist at approximately half frequency, out of which one is easily found with very favorable spatial matching (surface profiles of the pair of modes which are coupled in the experiment of Fig. 2, curve $a$, are shown in Figs. 3,4). Such occurrence is thus due to the simultaneous existence of a frequency range with numerous localized modes, together with the extended phonon regime at low frequencies (Fig. 1).

This is not the case for the periodical plate, where dispersion prevents good frequency matching between the fundamental and appropriate subharmonic modes. For the homogeneous plate the mismatch is due to the symmetry of fundamental modes: Only modes symmetric with respect to $x$ inversion (odd $n$) can induce a subharmonic, as apparent from Eq. (8), so that $\omega/2$ will never coincide with a plate eigenmode. In general, a detailed analysis of the factors contributing to $V_{\mathrm{th}}$ demonstrates that *the small frequency mismatch and large spatial overlap obtained for some modes of the Cantor-like sample cannot be simultaneously obtained in the ordered structures.*

In conclusion, we have given experimental evidence for low-threshold subharmonic generation in composites with Cantor-like code, and we have shown that its origin can be analyzed on the basis of the measured frequency and displacement profiles of the individual modes involved in the coupling. We have demonstrated that anomalously favorable conditions for anharmonic coupling may exist in fractal structures with respect to similar ordered structures, owing to the particular frequency distribution and spatial extension of normal modes. It cannot be excluded that similar conditions may occur in general disordered systems: Investigation of this point is in progress. We thus believe that our results may be of some importance

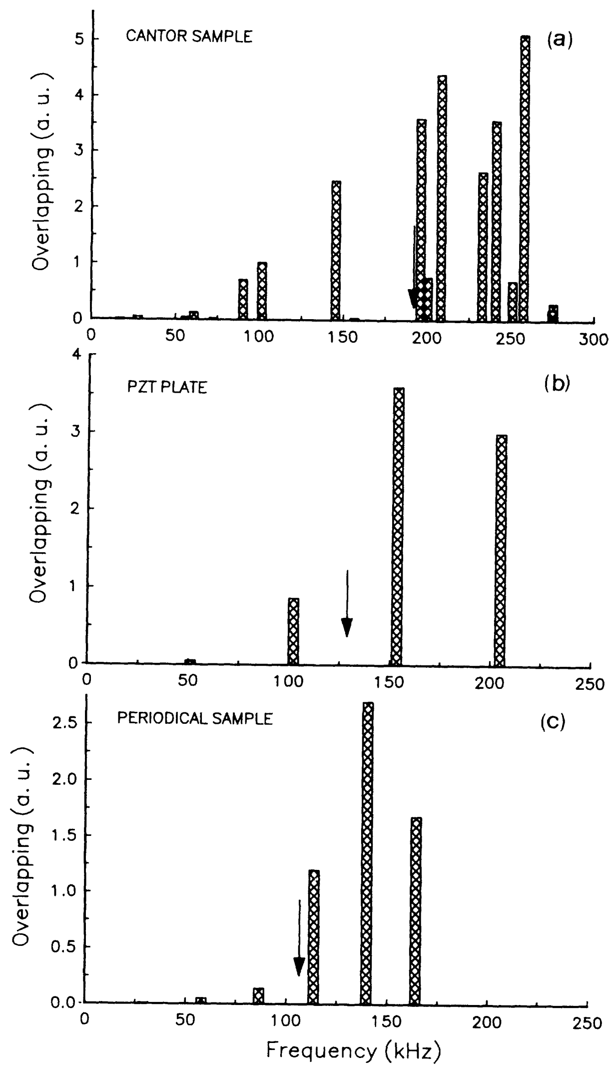


FIG. 5. Overlap integrals $I_o$, as defined in Eq. (8), for (a) the Cantor-like sample, (b) the homogeneous PZT, and (c) the periodical plate. The vertical arrow marks the frequency $\omega/2$.

to the study of nonlinearity in other classical or quantum wave phenomena.

We are grateful to R. Orbach for very useful discussions, to M. Breazeale for communicating data prior to publication, and to M. Acciarini for expert technical assistance. This work was supported in part by CNR, PF "Materiali speciali per tecnologie avanzate," and PF "Calcolo parallelo" (Grant No. 90.00658.PF69).

[(a)]Present and permanent address: Dipartimento di Fisica, Università di Modena, via Campi 213/A, I-41100 Modena, Italy. Phone: (39)59 586052. Electronic address (internet): MOLINARI at IMOVX2.UNIMO.IT FAX: (39)59 367488.

[1] See, e.g., the reviews by R. Orbach and by E. Courtens *et al.*, in *Fractals in Physics*, edited by J. Feder and A. Aharony (North-Holland, Amsterdam, 1990), pp. 266 and 41, and references therein.

[2] (a) A. Jagannathan, R. Orbach, and O. Entin-Wohlman, Phys. Rev. B **39**, 13465 (1989); (b) R. Orbach, Philos. Mag. B **65**, 289 (1992), and references therein.

[3] See, e.g., E. Atlee Jackson, *Perspectives of Nonlinear Dynamics* (Cambridge Univ. Press, Cambridge, 1991), Vol. I.

[4] See, e.g., L. Adler and M. A. Breazeale, J. Acoust. Soc. Am. **42**, 1152 (A) (1967); **48**, 1078 (1970).

[5] F. Delyon, Y.-E. Levy, and B. Souillard, Phys. Rev. Lett. **57**, 2010 (1986).

[6] F. Craciun, A. Bettucini, E. Molinari, A. Petri, and A. Alippi, Phys. Rev. Lett. **68**, 1555 (1992).

[7] See Ref. [2(b)]: "The one 'fly in the ointment' of our approach is the anomalously large value of the anharmonicity required to explain the agreement between theory and experiment."

[8] A. Alippi, F. Craciun, and E. Molinari, Appl. Phys. Lett. **53**, 1806 (1988); J. Appl. Phys. **66**, 2828 (1989).

[9] B. A. Auld, *Acoustic Fields and Waves in Solids* (Wiley Interscience, New York, 1973).

[10] The wave vector $q$ plotted on the horizontal axis is the wave vector relevant to each mode (thus, $q$ coincides with an effective wave vector for extended modes, but represents a "fracton wave vector" for localized modes) [6]. The superposition between different regimes is due to the fact that fracton modes resonant with the extended mode region may exist. The slope of the log-log curves in regions $b$ and $d$ is $\cong 1$, which corresponds to a spectral dimension $d_s = 0.63$ [6]. In Fig. 1 several theoretical points have no experimental counterpart: This is due to symmetry selection rules dictated by the excitation geometry [6,8].

[11] All plates had approximately the same total size. The ceramic elements in the periodical sample were similar in size to the smallest ceramic elements in the Cantor-like structure.

[12] A. Alippi, G. Shkerdin, A. Bettucci, F. Cracium, E. Molinari, and A. Petri (to be published).

[13] M. A. Breazeale (private communication).

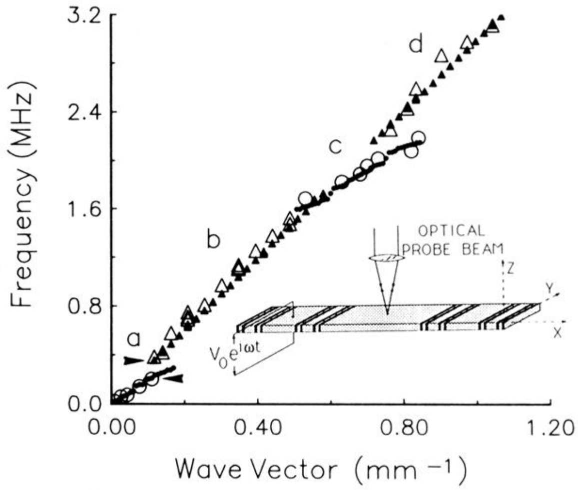


FIG. 1. Dispersion of the calculated (solid symbols) and the experimental (open symbols) normal modes of the Cantor-like sample sketched in the inset. Circles represent extended modes [phonon regimes (*a* and *c*)], while triangles represent localized modes [fracton regimes (*b* and *d*)]. For the definition of the wave vector $q$, see Ref. [10]. The arrows mark the modes involved in the anharmonic coupling (Fig. 2, curve *a*), whose experimental and theoretical displacement profiles are shown in Figs. 3 and 4.